

# Coordinated route planning of multiple fuel-constrained unmanned aerial systems with recharging on an unmanned ground vehicle for mission coverage

Subramanian Ramasamy<sup>†</sup> · Jean-Paul F. Reddinger<sup>‡</sup> · James M. Dotterweich<sup>‡</sup> · Marshal A. Childers<sup>‡</sup> · Pranav A. Bhounsule<sup>†</sup>

Received: date / Accepted: date

**Abstract** Small Unmanned Aerial Systems (sUAS) such as quadcopters are ideal for aerial surveillance because of their runway independence, terrain-agnostic maneuverability, low cost, and simple hardware. However, battery capacity constraints limit the effective range and endurance of sUASs, requiring human intervention to replace batteries or perform manual recharging for longer operations. To increase their range, an Unmanned Ground Vehicle (UGV) may provide recharging depot as needed. The problem is then to find optimal paths for the UGV and sUASs to visit mission points and sUAS-UGV rendezvous points for recharging. We present a three-tiered heuristics to solve this computationally hard combinatorial optimization problem: (1) K-means clustering is used to find UGV waypoints, (2) a traveling salesman formulation (TSP) is used to solve the optimal UGV route, and (3) vehicle routing problem formulation (VRP) with capacity constraints, time windows, and dropped visits is used to solve for sUAS routes. We use constraint programming for optimization of the TSP and VRP, achieving a solution for 25 mission points and up to 4 sUASs in about a minute on a standard desktop computer. We also found that constraint programming solvers are 7 – 30 times faster, but 4 – 15% sub-optimal compared to mixed-integer solvers, which provide exact solutions. Further, we used constraint programming solvers in a Monte-Carlo approach to evaluate the role of mission spread, number of clusters, and number of sUASs on the optimal solution. Our contribution is the development of heuristics for route selection of sUAS-UGVs that produces high quality solutions as more mission points and sUASs are added without substantially increasing the computational time.

---

This work was supported by ARO grant W911NF-14-S-003

<sup>†</sup> Subramanian Ramasamy and Pranav A. Bhounsule are with Dept. of Mechanical and Industrial Engineering, University of Illinois Chicago, IL, 60607 USA. E-mail: sramas21@uic.edu and E-mail: pranav@uic.edu

<sup>‡</sup> Jean-Paul F. Reddinger, James M. Dotterweich, Marshal A. Childers are with DEVCOM Army Research Laboratory, Aberdeen Proving Grounds, Aberdeen, MD 21005 USA. E-mail: jean-paul.f.reddinger.civ@army.mil and E-mail: james.m.dotterweich.civ@army.mil and E-mail: marshal.a.childers.civ@army.mil

**Keywords** Traveling Salesman Problem · Vehicle Routing Problem · K-means clustering · Fuel Constraints · Constraint Programming · Local Search Heuristics.

## 1 INTRODUCTION

1 Aerial vehicles such as quadcopters are ideally suited for missions such as surveil-  
 2 lance, reconnaissance, environment and traffic monitoring, search and rescue, and  
 3 border patrol [8]. Their relatively low cost, simple hardware, runway indepen-  
 4 dence, and terrain-agnostic maneuverability enables one to deploy several small  
 5 Unmanned Aerial Systems (sUASs) for large-scale area coverage [2]. However, a  
 6 key bottleneck is their limited battery capacity, which typically restricts them to  
 7 about 15 – 20 minutes of flight time [29].

8 The flight time and subsequently the coverage area of sUASs can be increased  
 9 by having several recharging depots spread across the area [17]. However, in non-  
 10 urban environments (e.g., rural areas) and in hostile environments (e.g., battle-  
 11 fields) it would be expensive or tactically impossible to have recharging depots  
 12 placed in advance [6]. A viable alternative is to have multiple sUASs recharge on  
 13 multiple Unmanned Ground Vehicles (UGV) that can provide sUAS recharging:  
 14 when the sUAS is low on fuel it coordinates with the UGV to find a rendezvous  
 15 point, lands on the UGV, recharges itself, and continues the mission.

16 Given a set of mission points, the number of sUASs, and the fuel-constraints  
 17 and other constraints on the speed and service time, the problem is to plan an  
 18 optimum route (e.g., minimum distance) for the sUAS and the UGV such that all  
 19 mission points are served and the sUASs never run out of battery charge. This is a  
 20 combinatorial optimization problem that is non-deterministic polynomial time or  
 21 NP-hard. Such problem can be solved in finite time by designing heuristics that are  
 22 problem dependent. This paper presents heuristics for planning the route of the  
 23 UGV and sUAS to achieve coordinate route planning while minimizing a suitable  
 24 objective (distance travelled by the sUASs) and meetings mission constraints (e.g.,  
 25 fuel constraints, service time constraints, vehicle speed constraints).

26 Khuller et al. [11] were the earliest ones to solve vehicle routing problem with  
 27 fuel constraints. They considered the problem of finding the cheapest route for a  
 28 fuel constrained vehicle with a set of fueling stations, each with a different fuel  
 29 price. They used a dynamic programming (DP) formulation to solve the problem.  
 30 Kannon et al. [10] considered the problem of finding the route of a fuel-constrained  
 31 aircraft to visit a set of waypoints with a set of aerial recharging waypoints. They  
 32 compared a mixed-integer linear programming (MILP) formulation with a DP  
 33 formulation and found that DP outperforms MILP.

34 Levy et al. [13] and Sundar et al. [27] considered extensions to multiple fuel-  
 35 constrained Unmanned Aerial Systems (sUASs). The goal here was to minimize the  
 36 distance travelled by multiple fuel-constrained sUASs to visit a set of waypoints  
 37 once and recharge on ground-based recharging depots. Levy et al. used a variable  
 38 neighborhood search based on randomization and variable neighborhood descent  
 39 based on the gradient to search for an optimal solution. Sundar et al. formulated  
 40 several mixed-integer linear programming (MILP) formulations and solved these  
 41 using an off-the-shelf MILP solvers. Similar to these works, Bung Duk Song et al.  
 42 [26] considered a multiple heterogeneous sUAS path planning problem in which  
 43 automatic Logistics Service Stations (LSS) are used for sUAS fuel replenishment.

44 Younghoon Choi et al. [33] implemented a new Coverage Path Planning (CPP)  
45 problem for solving the routes of a fleet of sUASs with energy constraints. The  
46 authors' novelty comes in formulating a column generation approach to deal with  
47 non-linear energy consumption, where traditional arc-based optimization approaches  
48 do not accurately estimate such function.

49 Radzki et al. [20] proposed a robust approach to delivery planning of small  
50 Unmanned Aerial Systems (sUAS) for disaster relief missions. The authors formu-  
51 lated an algorithm for planning of the routes of sUASs such a way that it ensures  
52 the proper execution of a certain delivery mission irrespective of any change in the  
53 weather conditions.

54 Andrew et al. [12] solved a two-tier route optimization problem of homoge-  
55 neous sUASs and repair vehicles for network exploration and failure repair. Their  
56 problem first solves for the optimal route of sUASs to explore the potential failure  
57 locations followed by the optimal route of repair vehicles to address the failure  
58 regions located by the sUASs.

59 Andres et al. [1] proposed a novel approach for global path optimization of  
60 sUASs by combining Traveling Salesman Problem and continuous optimal control  
61 formulations where the latter takes the sUAS dynamics and constraints into con-  
62 sideration. Sung et al., addressed the optimal zoning problem of Unmanned Aerial  
63 Vehicles using Genetic Algorithm to optimize package delivery services.

64 Maini et al. [15] considered the problem of routing a single fuel-constrained  
65 sUAS to a set of missions while being recharged by stopping at a UGV traveling  
66 on a road network. They solved the problem using a two-stage approach. First,  
67 using the sUAS range constraints, they found a set of recharging depots. Second,  
68 they formulated a mixed-integer linear program and solved for the path of both  
69 the sUAS and UGV. We consider an extension of the problem considered by Maini  
70 et al. These extensions are: we consider multiple fuel constrained sUASs, we use  
71 an off-road UGV, both of which add complexity to the problem as we need to plan  
72 the path of the UGV, the recharging points for the sUASs, and the paths for the  
73 sUASs.

74 We list some other works that are related to sUAS-UGV coordination in other  
75 settings and/or use clustering approach.

76 Manyam et al., [16] solved the problem of cooperative routing of sUAS-UGV  
77 to visit a set of mission points while being within a radius of each other to enable  
78 communication. They cast the resulting problem as a mixed integer programming  
79 problem and solved using a custom-written branch-and-bound algorithm. Petitprez  
80 et al., [19] considered deployment of sUAS and UGV such that the UGVs pick up  
81 sUASs that have land on fixed locations after visiting mission points. The objective  
82 was to minimize the operational cost while maximizing the inspection performance,  
83 a contradictory set of objectives that are solved using multi-objective optimization  
84 using genetic algorithms and capacitated arc routing problem. Their problem did  
85 not have a temporal aspect to it. Liu et al., [14] considered the problem of choosing  
86 recharge stations and flight routes for sUAS to visit given mission points. They  
87 cast the problem as a binary optimization problem, but solved it using heuristics  
88 that first cluster the mission points and then use local searches to solve for a  
89 path. Bard et al. [3] considered the problem of clustering a set of customers into  
90 zones such that a single vehicle can serve all the zones while meeting delivery and  
91 pick-up times. Since the pickup and delivery schedule is random, a probabilistic  
92 traveling salesman problem is formulated and solved using heuristics that break

93 the problem into two parts, solve them individually, and then connect back to  
 94 form the complete solution. Dondo et al., [5] used clustering approach to solve  
 95 a heterogeneous fleet vehicle routing problem with time windows. Initially, the  
 96 customers are clustered of customers based upon node locations, load, and time  
 97 windows. Then vehicles are assigned to the cluster followed by their sequencing.  
 98 Finally, the nodes within the cluster are ordered and arrival times are computed.  
 99 They used a standard mixed integer linear programming formulation which was  
 100 solved using branch and bound.

101 Multiple past researchers have considered the path planning of fuel-constrained  
 102 sUASs with fixed recharging stations. However, changing to a mobile recharging  
 103 station, a UGV in this case, adds a significant complexity to the problem. The  
 104 reasons are two-fold; one, the UGV path has to be planned and two, the sUAS-  
 105 UGV path is coupled. Our scientific contribution is the development of heuristics  
 106 to plan the UGV path and then use local search methods to compute sUAS paths  
 107 that ensures all constraints are met. Our heuristics enables us to decouple the  
 108 problems to an extent. It also enables us to add more sUASs or mission points  
 109 without substantial increase in the computation time.

110 Our main contribution is the solution of a relatively complex sUAS-UGV route  
 111 planning problem using heuristics.

- 112 1. We formulate a novel three-tier optimization: 1) K-means clustering to fix  
 113 UGV waypoints; 2) UGV route selection using a traveling salesman problem  
 114 formulation (TSP); and 3) sUAS route selection using a vehicle routing prob-  
 115 lem formulation (VRP) with capacity constraints (to enforce fuel limits), time  
 116 windows (to enable rendezvous with the UGV), and dropped visits (to allow  
 117 sUAS to visit the UGV at some locations and not all).
- 118 2. Use of OR-tools provides high quality solutions in relatively short times; we  
 119 solved upto 25 missions point, 1 UGV and 4 sUASs in about 60 seconds

120 We solve TSP and VRP using constraint programming within Google’s OR-  
 121 Tools<sup>TM</sup> framework [7]. The novelty of our work compared to previous work is  
 122 the formulation of heuristics to solve the coupled route planning problem that  
 123 includes multiple sUASs, fuel constraints, and travel and service constraints. Our  
 124 earlier work showed limited results on an example scenario involving 25 mission  
 125 points [23]. We expanded the current version to include 960 optimizations that  
 126 cover a range of mission distributions, number of sUASs, and cluster size. Our  
 127 heuristics enable us to achieve optimal solution under a minute on a standard  
 128 desktop computer. This opens up the possibility of real-time optimization during  
 129 practical implementation.

130 The rest of the paper is organized as follows: Section 2 introduces our coordi-  
 131 nated sUAS-UGV routing problem, followed by the formulation for optimizing the  
 132 ground vehicle route and aerial vehicle routes in a tiered fashion and the solution  
 133 approach to solve such problem. Section 3 presents the results obtained from solv-  
 134 ing such multi-tiered problem. Section 4 discusses the limitations present in our  
 135 model and how those will be addressed in the future research. The paper concludes  
 136 with Section 5.

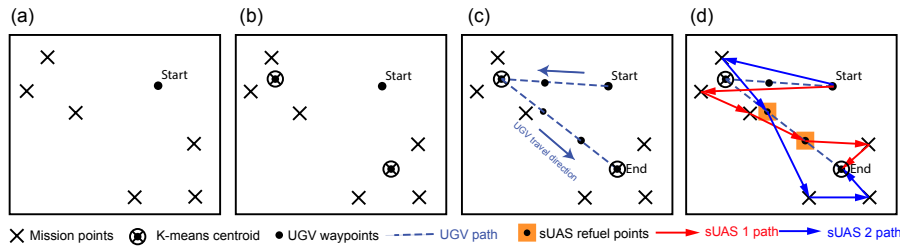


**Fig. 1** An overview of the problem and proposed solution: An example scenario is shown in (a). The problem is to get a pre-specified number of sUASs to travel over a set of mission points (shown by crosses). Due to fuel constraints, a single sUAS cannot cover all mission points and hence needs fuel depots which are provided by a moving UGV whose route also needs to be planned. A three-tiered solution is proposed. (b) Tier 1 - Find the centroids of the mission points using K-means clustering, (c) Tier 2- Use a traveling salesman problem formulation to plan the UGV route, and (d) Tier 3 - Use a vehicle routing problem formulation with time windows, capacity constraints, and dropped visits to plan the sUAS route.

## 137 2 METHODOLOGY

### 138 2.1 Overview of the problem and its solution

139 The overall objective is to plan the path of  $K$  fuel-limited Unmanned Air Vehi-  
 140 cles (sUASs) to pre-specified mission points while minimizing the total distance  
 141 travelled by all sUASs. The sUASs may be recharged by docking on a single Un-  
 142 manned Ground Vehicle (UGV). The path of the UGV and sUAS-UGV rendezvous  
 143 locations also needs to be computed. Fig. 1 (a) illustrates a typical scenario. The  
 144 mission locations (black cross marks) and the starting point ('start') of the UGV  
 145 and sUAS are pre-specified.

146 There are several constraints that need to be met. The velocity of the sUAS  
 147 is fixed and the velocity of the UGV is bounded. The sUAS battery capacity is  
 148 fixed, while the UGV has unlimited fuel. Since the velocity is constant, the battery  
 149 capacity of the sUAS is assumed to be directly proportional to the flight time. The  
 150 sUAS is assumed to dock on a stationary UGV during recharging and recharge  
 151 to full battery capacity. Both UGV and sUAS are stationary during recharging of  
 152 the sUAS. The recharging time of the sUAS is constant and is independent of the  
 153 remaining battery capacity.

154 We solve the problem in a tiered fashion: first we solve for the UGV route by  
 155 formulating and solving a traveling salesman problem and then the sUAS route  
 156 using vehicle routing problem formulation. Fig. 1 (a) shows the mission points  
 157 (crosses) and the start location for 2 sUASs and a single UGV. Because the sUASs  
 158 are fuel-constrained, they are unable to travel to all mission points. Thus, the  
 159 UGV path has to be planned so that it can provide recharging depots. As shown  
 160 in Fig. 1 (b), we use k-means clustering to find centroids for the mission points  
 161 (circle with a cross and a dot). Next, as shown in Fig. 1 (c), we use a traveling  
 162 salesman problem formulation to solve for the UGV route (blue dashed line) using  
 163 the centroids as nodes. We add more waypoints to the resulting path (black dots).  
 164 Finally, we formulate and solve a vehicle routing problem with capacity constraint  
 165 (to ensure we meet fuel constraints), time windows (to enable rendezvous with  
 166 the UGV), and dropped visits (to enable sUAS to drop visiting some of the UGV

**Algorithm 1** K-MEANS ALGORITHM

---

```

Input:  $k, [x_1, x_2, \dots, x_n]$ ;
1: Randomly place  $k$  centroid points  $c_1, c_2, \dots, c_k$ 
2: while not StoppingCondition() do
3:   for each observation  $x_i$  do
4:     evaluate nearest centroid point  $c_j$  by evaluating
       Euclidean distance  $\min \mathbf{D}(x_i, c_j)$ ;
5:     Assign observation  $x_i$  to the nearest centroid  $j$ ;
6:   end for
7:   for each do cluster  $j = 1, 2, \dots, k$ 
8:     recompute  $c_j = \frac{1}{n_j} \sum_{x_i \rightarrow c_j} x_i$ ;
9:   end for
10: end while

```

---

167 nodes). Thus, we can obtain the path of the 2 sUASs, including their recharging  
 168 spots on the UGV (orange square with black dot). Although we chose 2 clusters  
 169 for the k-means and 2 sUASs, it is unclear if this is the best choice. Hence, we vary  
 170 the number of clusters and sUASs and re-solve the problem to find their optimum  
 171 numbers for different spread or density of mission points.

172 **2.2 Problem Formulation**

173 We follow a three-tiered approach. First, we solve for waypoints for the UGV using  
 174 k-mean clustering (Sec. 2.2.1). Second, we solve for UGV route using a traveling  
 175 salesman problem formulation (Sec. 2.2.2). Third, we solve for sUAS route using  
 176 a vehicle routing problem formulation (Sec. 2.2.3).

177 *2.2.1 K-means clustering*

178 We use K-means clustering to find suitable waypoints for the UGV [32]. K-means  
 179 clustering is a technique to group  $n$  observations into  $k$  clusters. Each of these  $k$   
 180 clusters has a central location, which is the centroid of the cluster. Our goal is  
 181 to find the  $k$  centroids. This problem is NP hard, so we resort to the heuristic  
 182 Algorithm 1. We give a brief description of the algorithm.

183 The inputs to the algorithm are the ‘n’ mission locations  $x_1, x_2, \dots, x_n$  and the  
 184 number of clusters,  $k$ . Initially, we assign the centroid points at random. These  
 185 centroid points are assigned by picking some ‘k’ points randomly from location  
 186 of the existing mission points in the space. Next, we carry a sequential optimiza-  
 187 tion; first, to assign membership for an observation to a cluster, and second, to  
 188 recompute the centroid of the cluster. To assign membership, we find the distance  
 189 between an observation and centroid of each cluster and then assign the obser-  
 190 vation to the cluster with minimum distance. To recompute the centroid of the  
 191 cluster, we use the observations from the cluster. We repeat these two steps until  
 192 *StoppingCondition()* that no observation changes cluster membership.

193 *2.2.2 UGV route using traveling salesman formulation*

194 As described in the previous section, we have already found a sparse set of way-  
 195 points using k-means clustering. Using these waypoints as vertices, we formulate

196 and solve a Traveling Salesman Problem (TSP) find a route for the UGV. We  
 197 assume that the starting location of the UGV is pre-specified, but our algorithm  
 198 chooses the ending location. We assume that there is only a single UGV with  
 199 unlimited fuel capacity.

Consider a directed graph  $G' = (V', E')$  where  $V'$  is the entire set of vertices  
 $V' = \{0, 1, 2, \dots, k\}$ , which are the cluster centroids with 0 being the ‘start’ vertex,  
 and  $E'$  is the set of edges that gives the arc costs between  $i$  and  $j$  and  $E' =$   
 $\{(i, j) | i, j \in V', i \neq j\}$ . The  $c'_{ij}$  gives the non-negative arc cost between a particular  
 $i$  and  $j$ . The  $x'_{ij}$  is a binary variable where the value of  $x'_{ij}$  will be 1 if a vehicle  
 travels from  $i$  to  $j$ , and 0 otherwise. We formulate the TSP problem as follows,

$$\min \sum_{i \in V'} \sum_{j \in V'} c'_{ij} x'_{ij} \quad (1)$$

$$s.t., \sum_{i \in V'} x'_{ij} = 1, \quad \forall j \in V' \setminus \{0, k\} \quad (2)$$

$$\sum_{j \in V'} x'_{ij} = 1, \quad \forall i \in V' \setminus \{0, k\} \quad (3)$$

$$\sum_{j \in V'} x'_{0j} = \sum_{i \in V'} x'_{ik} = 1, \quad \{0, k\} \in V' \quad (4)$$

$$\sum_{i \in Q} \sum_{j \in Q} x'_{ij} \leq |Q| - 1, \quad \forall Q \subset \{1, \dots, k\}, |Q| \geq 2 \quad (5)$$

$$x'_{ij} \in \{0, 1\}, \quad \forall i, j \in V' \quad (6)$$

200 The objective in Eq. 1 is to minimize the total distance traveled by the UGV. The  
 201 constraints shown in Eq. 2 and Eq. 3 ensures that the UGV visits each vertex once,  
 202 that is, balancing the incoming and outgoing number of vehicles at a particular  
 203 vertex. Constraint in Eq. 4 ensures that the vehicle must start from a given ‘start’  
 204 vertex and ends at the ‘end’ vertex, that is, it does not loop back to the start  
 205 vertex. Although constraint Eq. 4 is satisfied by constraints Eq. 2 and Eq. 3, we  
 206 present them separately for the sake of completeness. Constraint in Eq. 5 ensures  
 207 that there are no sub-tours. Finally, constraint Eq. 6 represents the binary decision  
 208 variables.

### 209 2.2.3 sUAS routes using vehicle routing problem formulation

210 As described in the previous section, we have already found a path for the UGV.  
 211 Using this path, we assign a sufficient number of vertices on the path as possible  
 212 recharging depots for the sUAS-UGV rendezvous. We assume that each of the  
 213  $K$  sUASs starts at the same location as the UGV, formulate a vehicle routing  
 214 problem with capacity constraints to account for fuel limits, time windows to  
 215 allow for rendezvous, and dropped visits to allow the sUAS to visit some of the  
 216 many vertices on the UGV path. We constrain the sUAS to a fixed speed, pre-  
 217 specify the battery capacity and service time as the sUAS lands and waits on the  
 218 UGV.

219 The set of all UGV waypoints is denoted by  $D = \{0, 1, 2, \dots, m\}$ . There are  $n - m$   
 220 pre-specified mission points which belong to the set  $M = \{m + 1, \dots, n\}$ . The set of  
 221 all vertices is then  $V = M \cup D = \{0, 1, 2, \dots, m, m + 1, \dots, n\}$ . The set of all edges  
 222 denotes all possible connections between the vertices  $E = \{(i, j) | i, j \in V, i \neq j\}$ .

Consider a directed graph  $G = (V, E)$  where  $V$  is the entire set of vertices  $V = \{0, 1, 2, \dots, m, m+1, \dots, n\}$  and  $E$  is the set of edges that gives the arc costs between  $i$  and  $j$  and  $E = \{(i, j) | i, j \in V, i \neq j\}$ . Let  $c_{ij}$  be the non-negative arc cost between a particular  $i$  and  $j$ . Let  $x_{ij}$  be the binary variable where the value of  $x_{ij}$  will be 1 if a vehicle travels from  $i$  to  $j$ , and 0 otherwise. We formulate the VRP problem with fuel constraints, time windows, and dropped visits as follows,

$$\min \sum_{i \in V} \sum_{j \in V} c_{ij} x_{ij} \quad (7)$$

$$s.t., \sum_{i \in V} x_{ij} = 1, \quad \forall j \in M \setminus D \quad (8)$$

$$\sum_{j \in V} x_{ij} = 1, \quad \forall i \in M \setminus D \quad (9)$$

$$\sum_{i \in V} x_{ij} \leq 1, \quad \forall j \in D \setminus \{0\} \quad (10)$$

$$\sum_{j \in V} x_{ij} \leq 1, \quad \forall i \in D \setminus \{0\} \quad (11)$$

$$\sum_{j \in V} x_{0j} = \sum_{i \in V} x_{im} = K, \{0, m\} \in D \quad (12)$$

$$f_j \leq f_i - (c_{ij} x_{ij}) + L_1(1 - x_{ij}), \quad \forall i \in V, j \in V \setminus D \quad (13)$$

$$f_j = Q, \quad \forall j \in D \quad (14)$$

$$0 \leq f_j \leq Q, \quad \forall j \in V \quad (15)$$

$$t_j \geq t_i + (s_i + (c_{ij} x_{ij})) - L_2(1 - x_{ij}), \quad \forall i \in V, j \in V \quad (16)$$

$$t_j^l \leq t_j \leq t_j^u, \quad \forall j \in V \quad (17)$$

$$x_{ij} = 0, \quad \forall i \in D, \forall j \in D \quad (18)$$

$$x_{ij} = 1 \rightarrow f_i \geq c_{ij}, \quad \forall i \in V \setminus D, \forall j \in D \quad (19)$$

$$x_{ij} = 1 \rightarrow f_i = Q, \quad \forall i \in D, \forall j \in V \setminus D \quad (20)$$

$$x_{ij} = 1 \rightarrow \sum_{i \in V \setminus D} x_{ji} = 1, \quad \forall j \in D, \forall i \in V \setminus D \quad (21)$$

$$x_{mj} = 0, \quad \forall m \in D, \forall j \in V \quad (22)$$

$$x_{ij} \in \{0, 1\}, \quad \forall i, j \in V \quad (23)$$

$$f_i > 0, f_i \in \mathbb{R}_+ \quad \forall i \in V \quad (24)$$

$$t_i > 0, t_i \in \mathbb{Z} \quad \forall i \in V \quad (25)$$

$$s_i \geq 0, s_i \in \mathbb{Z} \quad \forall i \in V \quad (26)$$

$$Q > 0, \quad Q \in \mathbb{R}_+ \quad (27)$$

$$L_1, L_2 > 0, \quad L_1, L_2 \in \mathbb{R}_+ \quad (28)$$

223 The objective is Eq. 7 is to minimize the total distance traveled by the all the  
 224 sUASs. Constraints in Eq. 8 and Eq. 9 represents the flow conservation where  
 225 the inflow of a certain sUAS should be equal to the outflow of that sUAS at any  
 226 vertex among the mission vertices  $M$ . Constraints in Eq. 10 and Eq. 11 denotes  
 227 the optional stops the sUAS can take on the UGV vertices  $D$ , i.e., dropped visits.  
 228 Next, constraint in Eq. 12 also represents the flow conservation but here it is



229 represented for start and end vertices, where the number of sUASs leaving the  
 230 start vertex must be equal to the number of sUASs reaching the end vertex. The  
 231 start vertex and end vertex correspond to the first and last vertex of the UGV  
 232 route. The constraint in Eq. 13 is the Miller-Tucker-Zemlin (MTZ) formulation [18]  
 233 for sub-tour elimination. This constraint ensures that none of the sUAS batteries  
 234 are depleted out while eliminating sub-tours. In this constraint,  $L_1$  denotes a large  
 235 number. This constraint becomes active only when there is a flow between vertices  
 236  $i$  and  $j$  and subtracts from the sUAS fuel based on distance between the two  
 237 vertices. The fuel consumption of sUAS depends upon the distance traveled by  
 238 them. It is directly proportional to the distance traveled between two vertices  $i$   
 239 and  $j$ . Constraint Eq. 14 states that if the vertex is a recharging UGV stop,  
 240 then UGV has to refuel the sUAS to its full capacity  $Q$ . Constraint Eq. 15 is  
 241 the condition that the sUAS's fuel at any vertex in  $V$  should be between 0 and  
 242 maximum fuel capacity. Constraint Eq. 16 denotes that the cumulative arrival  
 243 time at  $j^{th}$  node is equal to the sum of cumulative time at the node  $i$ ,  $t_i$ , the  
 244 service time at the node  $i$ ,  $s_i$ , and the travel time between nodes  $i$  and  $j$ ,  $c_{ij}x_{ij}$ .  
 245 Here  $L_2$  denotes a large number which helps to eliminate sub-tour constraints  
 246 similar to Eq. 13. Constraint Eq. 17 is the time window constraint that the vehicle  
 247 visits a certain vertex in the specified time window for that node. In this problem,  
 248 the mission nodes are not constrained by time as the sUASs have the liberty to  
 249 visit those mission points that benefits them according to the travel of UGV. This  
 250 means that whenever sUAS needs to get refueled, it would be easier for it to go  
 251 to the UGV to refuel. Constraints Eq. 18 restricts that the two consecutive visits  
 252 made by the sUASs should not be consecutive UGV stops. Constraints Eq. 19 -  
 253 Eq. 21 represents the indicator constraints where the constraints to the right side  
 254 of the arrow should hold if the binary decision variable  $x_{ij}$  is equal to 1. If  $x_{ij}$  is  
 255 equal to zero, then the constraints to the right side of the arrow may be violated.  
 256 The constraint in Eq. 19 that if there is travel from any mission vertex  $i$  to the  
 257 UGV vertex  $j$ , then the fuel level at the  $i^{th}$  node should be atleast equal to the  
 258 distance traveled between them because the fuel consumption in this problem is  
 259 assumed to be linearly proportional to the distance traveled. Constraint in Eq. 20  
 260 indicates that if there is travel from the UGV vertex  $i$  to any mission vertex  $j$ ,  
 261 then the fuel level at the  $i^{th}$  node should be the maximum fuel capacity of the  
 262 sUAS as it is recharging to its full capacity at the UGV stop. The constraint in Eq.  
 263 21 makes sure that if any sUAS comes to the refuel vertex to recharge, then there  
 264 must exist an arc between that refuel node and a mission node to maintain the flow  
 265 conservation. Constraint in Eq. 22 denotes that there should not exist any flow  
 266 once the vehicle has reached the end node  $m$ . Eq. 23 is a binary decision variable  
 267 that is responsible for flow between the edges. Eq. 24 represents the continuous  
 268 decision variable that monitors the fuel level at any node and has zero as the lower  
 269 bound value. Eq. 25 represents the integer decision variable that computes the  
 270 cumulative time of sUAS's route and has zero as the lower bound. Eq. 26 denotes  
 271 the service time at the respective nodes, which is a positive integer with a lower  
 272 bound equal to zero. Eq. 27 represents the maximum fuel capacity of a sUAS  
 273 Finally, Eq. 28 denotes the large numbers used in the constraints Eq. 13 and Eq.  
 274 16.

**Table 1** Constraint Quantity analysis

Equation #	Number of constraints	Equation #	Number of constraints
8	$V - D$	16	$V^2$
9	$V - D$	17	$2 \times V^2$
10	$D - 2$	18	$D^2$
11	$D - 2$	19	$(V - D) \times D$
12	2	20	$(V - D) \times D$
13	$(V - D) \times V$	21	$((V - D) \times D) - (V - D)$
14	$D \times V$	22	$(V - D)$
15	$(2 \times (V - D)) \times V$		
$SUM = 6V^2 - 2D^2 + DV + 2V - 2$			

### 275 2.3 Solution using Constraint Programming (CP)

276 Table 1 gives an itemized lists the number of constraints in the sUAS problem  
 277 formulation. The equation numbers in the table correspond to the equations from  
 278 the Sec. 2.2.3. In the table, the notation  $V$  denotes the total number of vertices,  
 279 including all possible UGV stops and the mission points, while  $D$  denotes only the  
 280 UGV stops. The grand sum of all constraints  $SUM = 6V^2 - 2D^2 + DV + 2V - 2$ .  
 281 Thus, the number of constraints scale as the square of the number of mission  
 282 points.

283 We used Gurobi Mixed Integer Linear Programming (MILP) to solve for small  
 284 instances of this problem [9]. For  $k = 2$  clusters,  $D = 9$  and  $V = 34$  would give  
 285 a total constraint of 7146 and is solved about 40 sec using Gurobi on a standard  
 286 desktop (3.7 GHz Intel Core i9 processor with 32 GB RAM on a 64-bit operating  
 287 system). However, if  $k = 4$  then  $D = 17$  and  $V = 42$  would give constraints  
 288 of 10802 and is solved in 240 sec using Gurobi. Thus, Gurobi takes significantly  
 289 higher time as the number of constraints are increased. Thus, it does not scale  
 290 very well for a larger number of constraints.

291 Instead, we used Google’s OR-Tools<sup>TM</sup> to generate the results in this paper [7]  
 292 mainly for its speed of solution. OR Tools uses constrained programming (CP)  
 293 [24,25] to solve TSP and VRP problems. Constraint programming or constraint  
 294 optimization is a tool for solving hard combinatorial optimization problems by  
 295 searching for solutions that satisfy a list of constraints. Using Google’s OR-tools  
 296 for  $k = 2$  clusters and  $k = 4$  clusters as described earlier, required only 60 sec, and  
 297 the solution was about marginally better, about 4%, compared to Gurobi.

298 OR-Tools<sup>TM</sup> uses a search tree, local search, and meta-heuristics to find feasible  
 299 and, subsequently, the most optimal solutions. At the heart of OR-tools<sup>TM</sup> is a CP-  
 300 SAT solver [7]. The solver uses *DecisionBuilder* that has as its input, the decision  
 301 variables, rules to choose the next variable to assign a value, rules for choosing  
 302 the value to assign to the variable. Using the *DecisionBuilder*, we use the *Path*  
 303 *Cheapest Arc* strategy to find an initial feasible solution (see algorithm in [28]).  
 304 Starting with the “start” node, the decision builder connects the node that has the

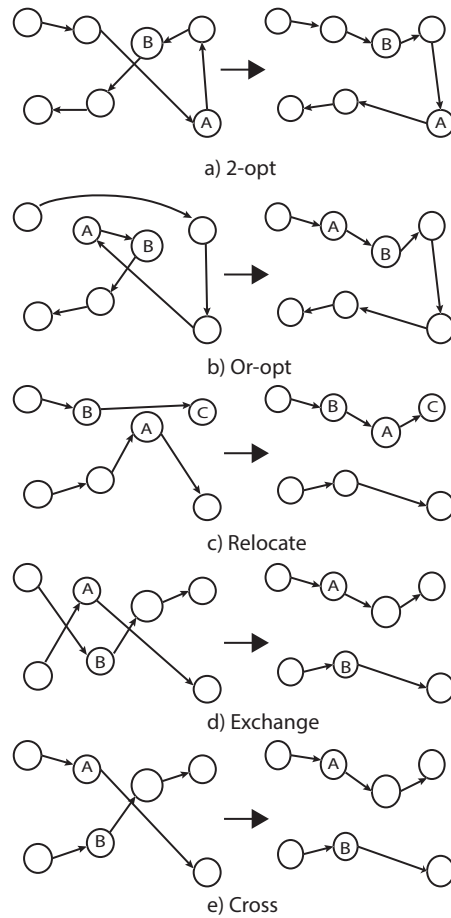


**Fig. 2** Move operators using in Constraint Programming [4]

305 shortest distance from the previous node and iterating till the end. While doing  
 306 the connections, it checks the feasibility of the solution.

307 Then OR-Tools<sup>TM</sup> uses a local search to find the best solution in the neighbor-  
 308 hood of the current solution.

309 This local search proceeds by a move operator that rewrites the nodes and checks  
 310 for feasibility and cost. These moves are repeated until a termination criteria, such  
 311 as no improvement of the objective. There are 5 move operators. These are listed  
 312 next and shown in Fig. 2 and is taken from [4].

- 313 1. **2-opt** interchanges the sub-part of a tour by removing two arcs, and then  
 314 connects them interchangeably so that the objective value gets reduced.
- 315 2. **Or-opt** moves the sub-part of a tour if there are a maximum of 3 contiguous  
 316 visits to that sub-part of the tour.
- 317 3. **Relocate** connects a visit of one tour to another tour if the reduction in  
 318 objective value is seen.

- 319 4. **Exchange** involves swapping two visits between each other from either the  
 320 same tour or two different tours.
- 321 5. **Cross** involves exchange of a visit at the end of one to another tour. The  
 322 difference between Exchange and Cross is that the Exchange move can be  
 323 done in any part of tour/tours, but Cross can be done only to the end portions  
 324 of two tours.

In order to escape a local optimum solution, OR-Tools<sup>TM</sup> use meta-heuristics. We use the Guided Local Search (GLS) in our problem [30]. In GLS, we add a penalty term to the objective function  $O$  leading to an augmented objective  $O'$  function. The penalty term is dependent on the neighborhood of the solution  $x$  through a set of features  $F$ . The augmented objective function is [4]

$$O'(x) = O(x) + \lambda \sum_{i \in F} f_i(x) p_i c_i \quad (29)$$

325 where the indicator function for the corresponding feature  $i$  that belongs to  $F$  is  
 326  $f_i$ . We define  $f_i(x) = 1$ , if the feature  $i$  is in solution or 0 otherwise. Also,  $\lambda$  is the  
 327 penalty factor that can tune the search for the solutions. For example, a larger  $\lambda$   
 328 increases the diversity of the solutions (also see [31]),  $p_i$  is the number of times the  
 329 particular feature  $i$  has been penalized, and  $c_i$  is the cost for the feature  $f_i$ . Using  
 330 the augmented objective  $O'$  increases the cost of the objective with respect to  
 331 the neighborhood, thus enabling the solver to get unstuck from a local optimum  
 332 solution. Subsequently, a local search is used to continue the search. For more  
 333 information about the implementation of OR-Tools and the flow of multi-tiered  
 334 optimization, we have uploaded a repository containing the simulation program in  
 335 Github [21].

### 336 3 RESULTS

337 We were interested in investigating how the distribution of mission points, the  
 338 number of clusters, and the number of sUASs affects the solutions of the coordi-  
 339 nates planning of sUAS-UGV routes. Figure 3 shows how the mission spread  
 340 was chosen. We chose 25 mission points over an area of  $8 \times 8$  kms, but vary the  
 341 mission spread. We started off with three cluster centroids randomly placed on  
 342 the map. Then we chose four densities ( $\rho$ ) for the mission points,  $\rho = 1, 2$  be-  
 343 ing clustered while  $\rho = 3, 4$  being uniformly spread out. For each density level  
 344  $\rho = 1, 2, 3, 4$ , we chose 20 different mission spreads. For each mission spread,  
 345 we optimized for clusters  $k = 2, 3, 4$  and sUASs  $K = 1, 2, 3, 4$ . Thus, we had  
 346  $4(\text{density}) \times 20(\text{mission spread}) \times 3(\text{clusters}) \times 4(\text{sUASs}) = 960$  optimization. All  
 347 the results are in Table 2.

348 In all optimizations, we enforce the following assumptions and constraints.  
 349 Each sUAS travels at a uniform speed of 10 m/s and has a total flight time of 15  
 350 min. Thus, each sUAS can travel 9 km between successive recharges. Hence, for  
 351 the area of  $8 \times 8$  kms, depending on the mission spread and number of sUASs, it  
 352 is possible to travel across all missions without a single recharge. There is a single  
 353 UGV in all optimization and it can vary its speed from 1.5 m/s to 4.5 m/s. The  
 354 time to recharge the sUAS once docked on the UGV, known as the service time,  
 355 is fixed at 5 min. Once the sUAS docks on the UGV, both of them don't move for  
 356 a time equal to the service time.

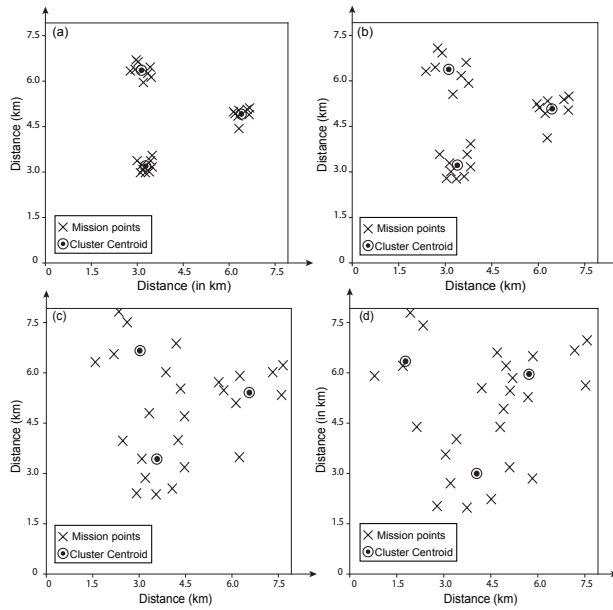


**Fig. 3** An example showing how density of mission locations was chosen. Three cluster centroids were chosen randomly. Keeping these centroids the mission points were spread out. Mission density is denoted by  $\rho$  (a)  $\rho = 1$  (most dense and clustered) (b)  $\rho = 2$  (clustered), (c)  $\rho = 3$  (spread out), and (d)  $\rho = 4$  (least dense and most spread out).

357 We used Constraint Programming (CP) solver in Google's OR-Tools<sup>TM</sup> to solve  
 358 both, the UGV route and the sUAS route. We used Python 3.9.4 and performed  
 359 the computations on a 3.7 GHz Intel Core i9 processor with 32 GB RAM on a  
 360 64-bit operating system. Each optimization took about 60 seconds, thus we could  
 361 do all 960 optimizations in about 16 min.

362 For a density  $\rho$  we choose 20 random position for the mission points and run  
 363 the optimization for a number of sUASs  $K$  and given cluster size  $k$ . Our metrics  
 364 for comparing the results for the 20 optimizations are the total distance covered by  
 365 all sUASs, the feasibility percentage, number of recharges, total time, and mission  
 366 time. The total distance is the sum of the distances travelled by all sUASs and  
 367 is the objective of the optimization. The feasibility percentage is the percentage  
 368 of feasible solutions out of 20 runs. The number of recharges is the total number  
 369 of recharges taken by all the sUASs. The total time is the sum of the travel and  
 370 service time for all sUASs. The mission time is the sum of the travel and service  
 371 time of the sUAS that takes the most time among all sUASs. Table 2 tabulates  
 372 the results using the above metric. We analyzed these results in more details in  
 373 Figs. 4 - 9.

374 Figures 4 compares the different metrics (distance, time, and recharging stops)  
 375 for sUASs for different mission densities. We assess the results for two sUASs,  
 376  $K = 2, 3$ . The metrics increase as the missions get more spread out with  $\rho = 1$   
 377 being most clustered and  $\rho = 4$  being least clustered. When comparing the different  
 378 sUASs, it can be seen that the total distance (a) and total time (c) are more for  
 379  $K = 3$  than  $K = 2$  while the total recharging stops (b) and mission time (d) are  
 380 less for  $K = 3$  than  $K = 2$ . Thus, more sUASs shorten the mission time at the  
 381 cost of increasing the travel distance.

**Table 2** Results for 960 optimization. Here  $K$  is the number of sUASs,  $\rho$  is the density of mission points with 1, 2 is clustered and 3, 4 is uniformly spread out,  $k$  is the number of clusters. Each row in the table, that is, for a given  $K$ , given density  $\rho$ , and given cluster  $k$ , corresponds to 20 optimizations. In each optimization there is randomization of mission points.

(a) Total distance (objective), feasibility percentage, and recharging stops

$K$	$\rho$	Total distance (in kms.)			Feasibility %			Total recharging stops		
		k=2	k=3	k=4	k=2	k=3	k=4	k=2	k=3	k=4
1	1	-	13.1±1.69	13.8 ± 1.8	0	55	65	0 ± 0	1 ± 0	1.38±0.48
	2	18 ± 0	16.4±2.09	19 ± 2.09	5	20	100	1 ± 0	1.75±0.43	2.75±0.83
	3	-	-	35 ± 4.34	0	0	90	0 ± 0	0 ± 0	4.83±1.17
	4	-	-	38.5±4.73	0	0	65	0 ± 0	0 ± 0	6.23±1.42
2	1	14.5±0.56	14.4±0.59	14.5±0.46	100	100	100	0.4 ± 0.49	0.4 ± 0.49	0.1 ± 0.3
	2	18.5±1.29	18.3±1.21	19.4±1.81	100	100	100	0.85±0.36	0.95±0.22	1.1 ± 0.83
	3	31 ± 4.45	31 ± 4.4	33 ± 8.95	35	85	95	2.57±1.05	2.77±0.94	3.3 ± 1.45
	4	33.8±2.73	36.9±7.49	37.5±5.95	20	80	95	3 ± 0.71	3.93±1.10	4.26±1.37
3	1	17.2±0.58	16.8±0.53	16.9±0.49	100	100	100	0 ± 0	0.2 ± 0.4	0.1 ± 0.3
	2	20.6±1.05	20.4±1.02	21.3±1.62	100	100	100	0.5 ± 0.5	0.75±0.54	0.75±1.04
	3	31.3±3.97	30.5±3.72	31.9±7.97	100	100	90	1.65±0.79	1.85±0.91	2.17±0.83
	4	37.6±5.97	35.8±6.84	38.8±7.93	100	100	90	2.3 ± 0.95	2.65±1.15	3.56±1.30
4	1	20 ± 0.53	19.3 ± 0.6	19.5±0.51	100	100	100	0.2 ± 0.4	0.4 ± 0.49	0.1 ± 0.3
	2	23.3 ± 1.1	23.1±1.16	24.1±1.56	100	100	100	0.45±0.50	0.55±0.50	0.8 ± 1.03
	3	32.9±4.17	33.6±3.51	34.9±4.46	100	100	90	1.65±1.01	1.95±0.86	1.94±0.78
	4	37.8±5.48	36.7±5.61	38.1±6.68	100	95	75	1.65±1.11	1.89±1.12	2.53±1.50

(b) Total time and mission time

$K$	$\rho$	Total time (in min.)			Mission time (in min.)		
		k=2	k=3	k=4	k=2	k=3	k=4
1	1	-	163.7 ± 6.02	169.18 ± 9.1	-	163.7 ± 6.02	169.18 ± 9.1
	2	165.72 ± 0	171.03 ± 6.98	192.27 ± 8.58	165.72 ± 0	171.03 ± 6.98	192.27 ± 8.58
	3	-	-	230.37±12.39	-	-	230.37±12.39
	4	-	-	242.82±14.39	-	-	242.82±14.39
2	1	161.43 ± 3.67	161.23 ± 3.64	160.21 ± 4.09	93.36 ± 14.96	98.63 ± 22.40	89.48±416.08
	2	171.29 ± 5.91	173.78 ± 4.84	178.66 ± 9.81	107.92±12.07	121.24±18.48	116.82±22.11
	3	205.68±15.35	208.52±14.56	208.08±50.77	117.95 ± 7.07	141.06±10.64	157.62±45.54
	4	214.05 ± 8.34	224.92±21.56	230.19±16.56	119.05 ± 3.98	136.44±12.95	190.32±25.26
3	1	168.28 ± 0.97	170.27 ± 3.84	67.99 ± 5.18	168.28 ± 0.97	88.36 ± 19.85	76.68 ± 16.31
	2	177.94 ± 4.26	179.77 ± 3.84	182.27±10.61	91.19 ± 19.37	111.13±28.31	95.39 ± 31.21
	3	202.60±12.40	205.53±13.86	212.77±13.94	90.04 ± 8.43	118.12±28.31	135.35±27.61
	4	219.23±14.99	219.57±19.04	233.91±19.77	98.91 ± 13.64	124.52±18.10	166.09±32.66
4	1	168.20±33.11	180.21 ± 3.58	178.64 ± 4.17	78.65 ± 35.78	89.69 ± 21.99	78.65 ± 33.18
	2	186.21±4.315	187.69 ± 5.54	192.61±11.16	84.58 ± 20.18	101.61±29.47	94.27 ± 31.91
	3	211.20±13.77	215.19±11.29	219.42±13.10	90.37 ± 10.10	113.84±19.98	116.56±30.68
	4	219.30±15.84	219.52±16.02	229.52±20.02	94.31 ± 10.51	112.15±21.02	137.69±41.12

382 Fig. 5 depicts four distributions of mission points, with decreasing density from  
383 (a) to (d). We use cluster size  $k = 3$  for computing UGV route and  $K = 2$  sUASs  
384 to serve the mission points. Since the cluster centroids are at the same location  
385 for all cases, the UGV route, including its distance, remains the same. We show  
386 the metrics in the side box in each figure. We can see that for (a) and (b) with  
387  $\rho = 1, 2$  (most dense) have lower values for the 4 metrics when compared with (c)  
388 and (d) with  $\rho = 3, 4$ . Clearly, as the missions get spread out, the sUASs have to  
389 travel a larger distance, which increases the number of recharging stops, the total  
390 time, and the mission time.

391 Figures 6 compares the different metrics (distance, time, and recharging stops)  
392 for different cluster size in the K-mean clustering. We present results for two  
393 different densities  $\rho = 2$  (clustered) and  $\rho = 3$  (uniformly spread) for 3 sUASs. The

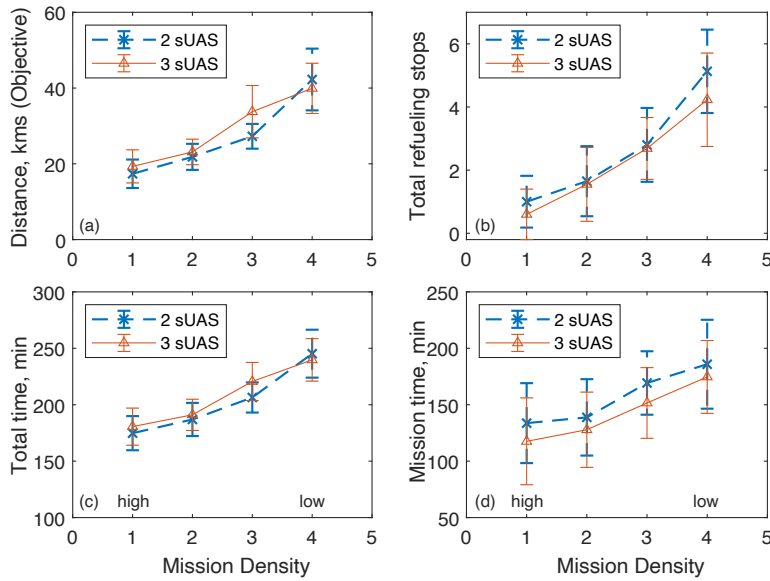


**Fig. 4** Metrics as function of mission density for 2 and 3 sUASs: (a) Total Distance (objective), (b) Total recharging stops, (c) Total time, (d) Mission time, all as a function of density  $\rho$  from  $\rho = 1, 2$  (missions are clustered) to  $\rho = 3, 4$  (missions are uniformly spread out).

394 metrics increase as the density changes from clustered  $\rho = 2$  to uniformly spread  
 395 out  $\rho = 3$  as expected. The clusters size  $k$  does not seem to show a correlation for  
 396 highly clustered missions. For instance, for density level  $\rho = 2$ , the total distance  
 397 and total time are almost the same for different cluster sizes, while the recharging  
 398 stops and mission time show an increase for  $k = 3$ . The clusters size  $k$  seems to  
 399 show some correlation for spread out missions. For instance, for density level  $\rho = 3$ ,  
 400 the total distance decreases, but the total time, mission time, and recharging stops  
 401 all increase with an increase in the cluster size.

402 Fig. 7 (a) shows the mission points for one scenario with density of  $\rho = 3$ .  
 403 We chose different cluster sizes for the k-mean clustering. The plots (a), (b), and  
 404 (c) correspond to  $k = 2, 3, 4$  respectively. We can observe that the UGV route  
 405 increases as  $k$  increases. We then solve each scenario with the same number  $k = 3$   
 406 sUASs. We note that the total distance (objective) is almost the same for all three  
 407 optimizations. The recharging stops and the total time for  $k = 2$  (b) and for  $k = 3$   
 408 (c) are almost the same, while those for  $k = 4$  are slightly higher. The extra total  
 409 time for  $k = 4$  is probably because of the added recharging stop, which adds a  
 410 service time to the total time. Finally, the mission time increases across from (b)  
 411 to (d) because of the unequal sharing of missions as the cluster size increases.

412 Figures 8 compares the different metrics (distance, time, and recharging stops)  
 413 for different number of sUASs. We use two density levels,  $\rho = 1, 2$  (both clustered)  
 414 and chose a cluster size of  $k = 3$ . The metrics increase as the density decreases  
 415 from  $\rho = 1$  to  $\rho = 2$  as expected. As the number of sUASs increase, the total  
 416 distance (objective) (a) and total time (c) increases while the recharging stops (b)  
 417 and the mission time (d) decreases. We may attribute the reduction in these latter  
 418 metrics to better sharing of the missions among the sUASs.

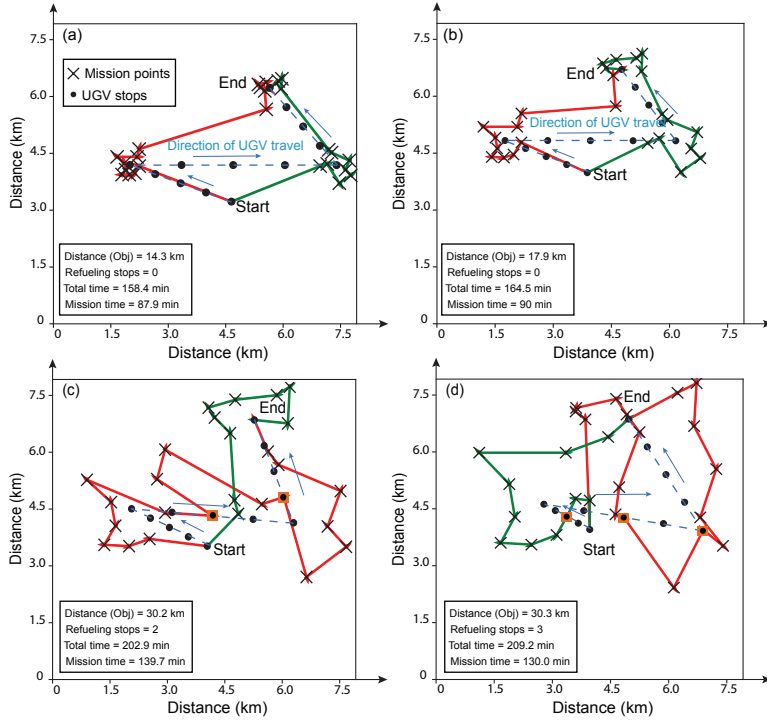


**Fig. 5** Optimizations illustrating the solution for a mission density changes. Here cluster  $k = 3$  and sUAS  $K = 2$ . The mission densities are (a)  $\rho = 1$  (dense and clustered), (b)  $\rho = 2$  (less dense than  $\rho = 1$ , but clustered), (c)  $\rho = 3$  (uniformly spread out),  $\rho = 4$  (uniformly spread out with spread greater than  $\rho = 3$ )

419 Fig. 9 shows the solution obtained by changing the number of sUASs for the  
 420 same distribution of mission with density  $\rho = 2$  and cluster size  $k = 3$ . Since  
 421 the density and cluster size are the same, the UGV route is the same across all  
 422 scenarios. The overall distance and total time increases, and the refueling stops and  
 423 mission times decreases with the increase in the number of sUASs. The increase  
 424 in total distance with increase in sUASs may be attributed to inefficient sharing  
 425 of missions, which also increases the total time. However, the benefit of inefficient  
 426 sharing is that recharging stops decrease, which also reduces the mission time.

#### 427 4 DISCUSSION

428 In this paper, we have presented heuristics for planning the path of a multiple  
 429 fuel-constrained small Unmanned Aerial Systems (sUASs) and a single Unmanned  
 430 Ground Vehicle (UGV) such that the sUASs can visit a set of mission points while  
 431 minimizing the total distance covered and without running out of fuel by docking  
 432 on the UGV to recharge. We solved the problem in a tiered fashion; first, we use the  
 433 mission points to create waypoints for the UGV using K-means clustering; second,  
 434 we solved for the UGV route using the Traveling Salesman Problem formulation



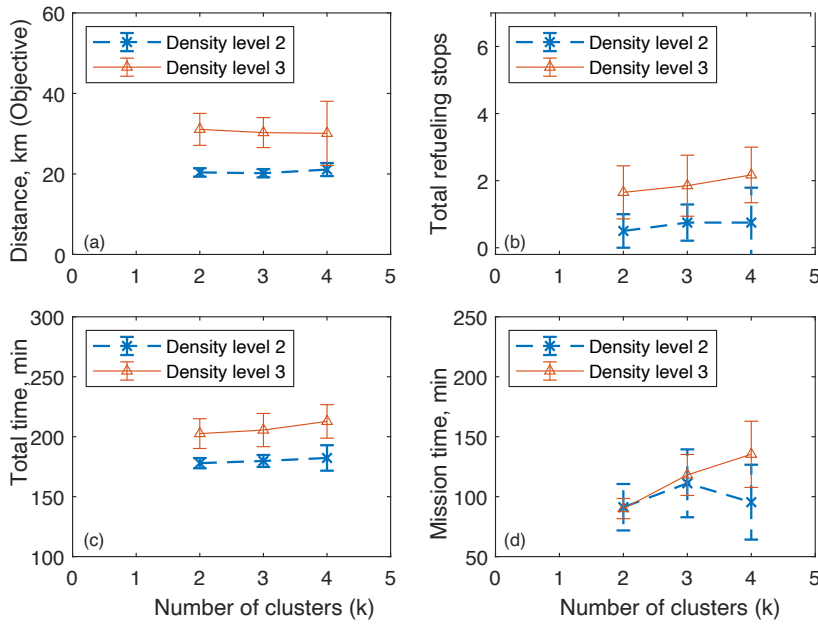


**Fig. 6** Metrics as function of number of clusters for 3 sUASs for two density levels  $\rho = 2$  is clustered and  $\rho = 3$  is uniformly spread out. (a) Total Distance (objective), (b) Total recharging stops, (c) Total time, (d) Mission time, all as a function of number of clusters.

435 using the waypoints as vertices; third, we solved for the sUAS route by using  
 436 mission points and using waypoints on the path of the UGV as vertices and using  
 437 a Vehicle Routing Problem formulation with capacity constraints (fuel limits),  
 438 time windows (to match UGV rendezvous points for recharging), and dropped  
 439 visits (to allow sUAS to drop some of the rendezvous points).

440 We solved the mixed integer programming problem (MILP) formulated in  
 441 Sec. 2.2.3 using constraint programming which is based on heuristics. The same  
 442 problem may be solved using MILP solvers such as Gurobi [9]. We compared so-  
 443 lutions obtained by both solvers in a limited number of cases and the results are  
 444 shown in Tab. 3. Each row in the table corresponds to a certain setting given by  
 445 the number of sUAS's ( $K$ ), the mission density ( $\rho$ ), and the cluster size  $k$ . For  
 446 each setting, we choose 10 scenarios and run the optimization. The table gives the  
 447 objective value and the optimization time for each solver. The optimality gap is  
 448 the percent difference in the objective value between OR-Tools and Gurobi. It can  
 449 be seen that Gurobi is between 4 – 15% more optimal than OR-tools. However,  
 450 while OR-Tools takes a maximum of 10 seconds (which is the termination crite-  
 451 ria for the optimization), Gurobi takes between 71 – 300 seconds, indicating the  
 452 computational superiority of using OR-Tools. Thus, we conclude that OR-Tools  
 453 is 7 – 30 times faster than Gurobi, but only 4 – 15% sub-optimal. Hence, we used  
 454 OR-Tools in our calculations.

455 We make some general observations based on our limited study of 25 mission  
 456 points with at least one mission point beyond the coverage area of a single sUAS.  
 457 The spread of the mission points is an important criteria that affects the solution

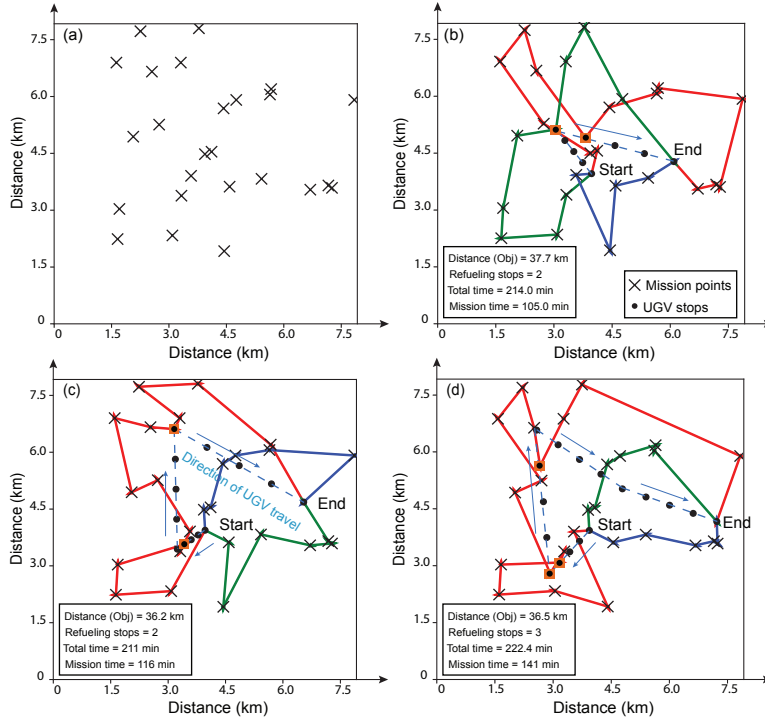


**Fig. 7** Optimizations illustrating the solution different cluster sizes. Here mission density  $\rho = 3$  and sUAS  $K = 3$ . The spread of missions is shown in (a). The cluster sizes are (b)  $k = 2$ , (c)  $k = 3$ , and (d)  $k = 4$

458 feasibility and the nature of optimal solution. When the missions are well clustered  
 459 ( $\rho = 1, 2$  here), we find feasible solutions with  $K \geq 2$  sUASs, but as the missions  
 460 spread out ( $\rho = 3, 4$ ), we need  $K \geq 3$  sUASs to serve all mission points. The results  
 461 suggest that there is a minimum number of sUASs to generate feasible solutions  
 462 which depend on the mission spread and the fuel level.

463 The number of sUASs has a strong correlation with the optimization outcomes.  
 464 The total distance travelled by all sUASs increases as the number of sUASs in-  
 465 creases. This is because multiple sUASs are now sharing mission points closer  
 466 to each other, resulting in a larger travel distance. The increased total distance  
 467 leads to larger total travel time. However, the maximum distance travelled by any  
 468 given sUAS is smaller, which correlates to a shorter mission time. The number of  
 469 recharging stops also decreases as more sUASs have a bigger collective range.

470 The cluster size chosen shows a weak correlation with the outcomes. For a  
 471 given density and number of sUASs, the total distance covered, recharging stops,  
 472 total time, and mission time remained almost constant.

473 We have not shown solutions for a single cluster  $k = 1$  and multiple sUASs  
 474  $K = 1, 2, 3, 4$ . This is because we end up with very few feasible solutions and hence  
 475 should be avoided. The  $k = 1$  cluster size leads to a rather restrictive UGV route  
 476 that prevents the VRP formulation from finding feasible solutions.

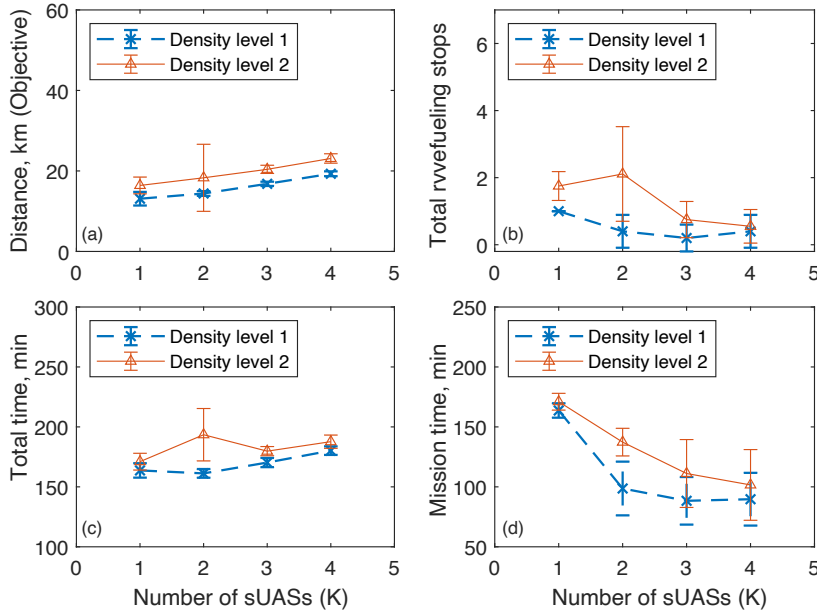


**Fig. 8** Metrics as function of number of sUASs for cluster size of 3 for two density levels, both of which correspond to clustered distributions. (a) Total Distance (objective), (b) Total recharging stops, (c) Total time, (d) Mission time, all as a function of number of sUASs.

**Table 3** Comparison between constraint programming solver (OR-tools) and mixed-integer linear programming solver (Gurobi). Each row corresponds to particular combination of  $K$ ,  $\rho$ , and  $k$  where  $K$  represents the number of sUAS,  $\rho$  represents the mission density, and  $k$  represents the number of clusters. These are for 10 randomly chosen scenarios for each row. The optimality gap is the percent error between Gurobi and OR-tools

Mission distribution pattern	Gurobi		OR-Tools		Optimality gap (%)
	Objective value (in km.)	Optimization time (in s)	Objective value (in km.)	Optimization time (in s)	
K=1, $\rho=2, k=4$	17.15 ± 0.85	300 ± 0	20.41 ± 1.23	10 ± 0	15.5 ± 5.80
K=2, $\rho=3, k=3$	27.99 ± 2.89	155.8 ± 135.52	30.04 ± 4.19	10 ± 0	8.37 ± 5.42
K=3, $\rho=3, k=3$	29 ± 2.77	71.3 ± 117.96	30.59 ± 3.76	10 ± 0	4.9 ± 4.14
K=4, $\rho=4, k=2$	35.95 ± 3.15	117.2 ± 76.26	37.79 ± 4.11	10 ± 0	4.3 ± 4.17

477 The key advantage of our framework is the decomposition of a complex prob-  
 478 lems into three-stages. This simplifies the problem formulation. The use of con-  
 479 straint programming as a solver gives high quality solution in fraction of seconds  
 480 for the scenarios considered here (25 missions points, 1-4 sUAS an 1 UGV).

481 The prime disadvantage of our tiered heuristics is the cascading effect of pa-  
 482 rameter choices. In our case, the quality of the k-means clustering determines the  
 483 UGV route, which then determines the sUAS route. Thus, a poor choice of cluster  
 484 size can affect the final solution. We can see this for  $K = 1$  and  $k = 2, 3$  where  
 485 we get no feasible solution. The K-mean clustering and UGV route selection do

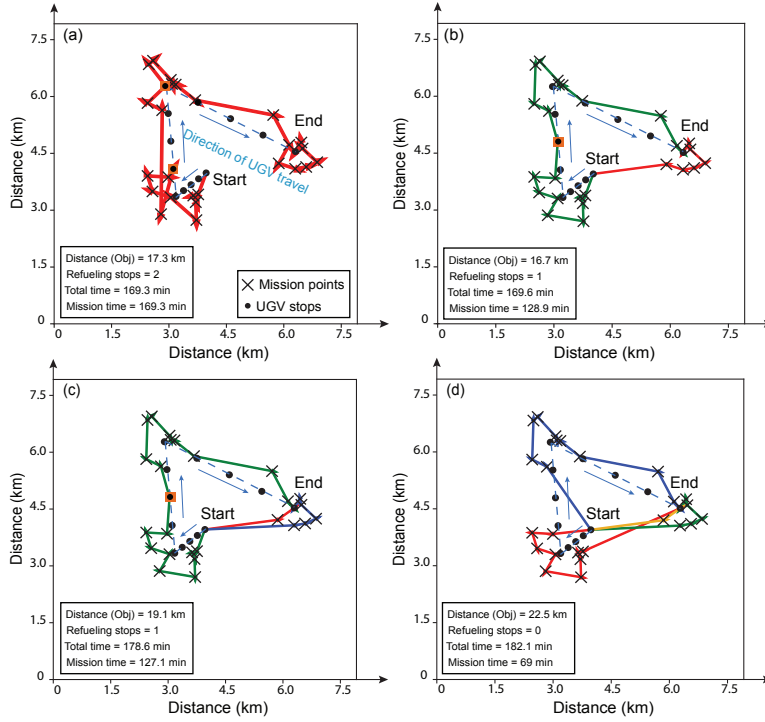


**Fig. 9** Optimizations illustrating the solution for different number of sUASs. Here mission density  $\rho = 2$  and cluster size is  $k = 3$ . The number of sUASs are (a)  $K = 1$ , (b)  $K = 2$ , (c)  $K = 3$ , and (d)  $K = 4$ .

486 not consider the number of mission points in a cluster. If there are more mission  
 487 points in a cluster than we should probably give that cluster a higher preference  
 488 to be visited earlier than later. As the number of sUASs increases, we notice that  
 489 there is unequal sharing of mission points (e.g., Fig. 9 (d)). There are probably  
 490 two reasons for this: one, the geographic distribution of the missions favors this  
 491 solution, and two, we did not enforce that all sUASs finish their missions simulta-  
 492 neously, thus allowing some sUASs to travel a shorter distance. We have overcome  
 493 this issue to an extent by using genetic algorithms and bayesian optimization to  
 494 tune the parameters [22].

495 We finish by listing directions for future work. We assumed fixed recharging  
 496 time for sUAS irrespective of its existing fuel level before recharging. This is not  
 497 optimal. Thus, future research address this issue in such a way that the refueling  
 498 amount, and thereby the refueling time, of the sUAS on UGV depends upon  
 499 the existing fuel level before any sUAS reaches the UGV from a mission to get  
 500 recharged. We have assumed that UGV has indefinite fuel capacity which is not  
 501 the case in practical scenarios. Future studies will consider fuel capacity of the  
 502 UGV. Furthermore, the terrain chosen affects the UGV fuel usage and it will also  
 503 need to be taken into account in solving the routing problem.

## 5 CONCLUSION

We conclude that the problem of routing multiple fuel-constrained small Unmanned Aerial Systems (sUAS) with recharging on a single Unmanned Ground Vehicle (UGV) can be solved quickly and efficiently using a tiered heuristics where the UGV route is solved first followed by the sUAS route within a constraint programming approach. We can solve routes for about 25 mission points with 1 to 4 sUAS and a single UGV in less than a minute on standard desktop computer. This opens up the possibility of real-time optimization during practical implementation. Our main observations are: (1) there is a minimum number of sUASs needed based on the fuel constraints and velocities of the sUAS and UGV and mission spread, and (2) the number of clusters need to be  $k > 1$ , but there is no clear correlation between cluster size and the solution. The overall distance and overall time taken increases as the missions spread out and as the number of sUASs increase. However, the mission time and the recharging stops decrease as the number of sUASs increases. Finally, we found that constraint programming solvers are 7 – 30 times faster, but 4 – 15% sub-optimal compared to mixed-integer solvers, which provide exact solutions.

## Declarations

- Funding: The work by SR and PAB was funded by Army Research Laboratory grant W911NF-14-S-003.
- Conflict of interest/Competing interests: The authors declare no conflict of interest.
- Code or data availability: [https://github.com/Subram0212/JINT\\_paper\\_codes](https://github.com/Subram0212/JINT_paper_codes)
- Authors' contributions: Conceptualization, SR, JPR, JD, CM, PAB; methodology, SR and PAB; software and validation, SR; writing—original draft preparation, SR and PAB; writing—review and editing, JPR, JD, CM, PAB; supervision, JPR, JD, CM, PAB; project administration, PAB. All authors have read and agreed to the published version of the manuscript.'
- Ethics approval: Not applicable.
- Consent to participate: Not applicable.
- Consent for publication: All authors consent to publication.

## References

1. Albert, A., Immsland, L.: Combined optimal control and combinatorial optimization for searching and tracking using an unmanned aerial vehicle. *Journal of Intelligent & Robotic Systems* **95**(2), 691–706 (2019)
2. Altshuler, Y., Pentland, A., Bruckstein, A.M.: Optimal dynamic coverage infrastructure for large-scale fleets of reconnaissance UAVs. In: *Swarms and Network Intelligence in Search*, pp. 207–238. Springer (2018)
3. Bard, J.F., Jarrah, A.I., Zan, J.: Validating vehicle routing zone construction using monte carlo simulation. *European Journal of Operational Research* **206**(1), 73–85 (2010). DOI <https://doi.org/10.1016/j.ejor.2010.01.045>. URL <https://www.sciencedirect.com/science/article/pii/S0377221710001049>
4. De Backer, B., Furnon, V., Shaw, P., Kilby, P., Prosser, P.: Solving vehicle routing problems using constraint programming and metaheuristics. *Journal of Heuristics* **6**(4), 501–523 (2000)

- 549 5. Dondo, R., Cerdá, J.: A cluster-based optimization approach for the multi-depot hetero-  
550 geneous fleet vehicle routing problem with time windows. *European journal of operational*  
551 *research* **176**(3), 1478–1507 (2007)
- 552 6. Freed, M., Fitzgerald, W., Harris, R.: Intelligent autonomous surveillance of many targets  
553 with few UAVs. In: *Proceedings of the Research and Development Partnering Conference*,  
554 Department of Homeland Security, Boston, MA (2005)
- 555 7. Google: Google OR-tools. <https://developers.google.com/optimization> (2021). On-  
556 line; accessed Feb 2, 2021
- 557 8. Griffiths, S.R.: *Remote terrain navigation for unmanned air vehicles* (2006)
- 558 9. Gurobi: Gurobi Optimization LLC. <https://www.gurobi.com/> (2021). Online; accessed  
559 Sep 19, 2021
- 560 10. Kannon, T.E., Nurre, S.G., Lunday, B.J., Hill, R.R.: The aircraft routing problem with  
561 refueling. *Optimization Letters* **9**(8), 1609–1624 (2015)
- 562 11. Khuller, S., Malekian, A., Mestre, J.: To fill or not to fill: The gas station problem. *ACM*  
563 *Transactions on Algorithms (TALG)* **7**(3), 1–16 (2011)
- 564 12. Lee, A.C., Dahan, M., Weinert, A.J., Amin, S.: Leveraging suavs for infrastructure network  
565 exploration and failure isolation. *Journal of Intelligent & Robotic Systems* **93**(1-2), 385–  
566 413 (2019)
- 567 13. Levy, D., Sundar, K., Rathinam, S.: Heuristics for routing heterogeneous unmanned vehi-  
568 cles with fuel constraints. *Mathematical Problems in Engineering* **2014** (2014)
- 569 14. Liu, Y., Liu, Z., Shi, J., Wu, G., Chen, C.: Optimization of base location and patrol  
570 routes for unmanned aerial vehicles in border intelligence, surveillance, and reconnaissance.  
571 *Journal of Advanced Transportation* **2019** (2019)
- 572 15. Maini, P., Sundar, K., Rathinam, S., Sujit, P.: Cooperative planning for fuel-constrained  
573 aerial vehicles and ground-based refueling vehicles for large-scale coverage. arXiv preprint  
574 arXiv:1805.04417 (2018)
- 575 16. Manyam, S.G., Casbeer, D.W., Sundar, K.: Path planning for cooperative routing of air-  
576 ground vehicles. In: *2016 American Control Conference (ACC)*, pp. 4630–4635 (2016).  
577 DOI 10.1109/ACC.2016.7526082
- 578 17. Mersheeva, V.: UAV routing problem for area monitoring in a disaster situation. Ph.D.  
579 thesis, PhD thesis (2015)
- 580 18. Miller, C.E., Tucker, A., Zemlin, R.A.: Integer programming formulation of traveling sales-  
581 man problems. *J. ACM* **7**, 326–329 (1960)
- 582 19. Petitprez, E., Georges, F., Raballand, N., Bertrand, S.: Deployment optimization of a fleet  
583 of drones for routine inspection of networks of linear infrastructures. In: *2021 International*  
584 *Conference on Unmanned Aircraft Systems (ICUAS)*, pp. 303–310 (2021). DOI 10.1109/  
585 ICUAS51884.2021.9476674
- 586 20. Radzki, G., Golinska-Dawson, P., Bocewicz, G., Banaszak, Z.: Modelling robust delivery  
587 scenarios for a fleet of unmanned aerial vehicles in disaster relief missions. *Journal of*  
588 *Intelligent & Robotic Systems* **103**(4), 1–18 (2021)
- 589 21. Ramasamy, S.: Uav-ugv routing code. [https://github.com/Subram0212/JINT\\_paper\\_](https://github.com/Subram0212/JINT_paper_codes)  
590 [codes](https://github.com/Subram0212/JINT_paper_codes) (2022). Online; accessed Feb 13, 2022
- 591 22. Ramasamy, S., Md, M., Reddinger, J.P.F., Dotterweich, J.M., D., H.J., Childers, M.A.,  
592 Bhounsule, P.A.: Heterogenous vehicle routing: comparing parameter tuning using genetic  
593 algorithm and bayesian optimization. In: *2022 International Conference on Unmanned*  
594 *Aircraft Systems (ICUAS)* (2022)
- 595 23. Ramasamy, S., Reddinger, J.P.F., Dotterweich, J.M., Childers, M.A., Bhounsule, P.A.:  
596 Cooperative route planning of multiple fuel-constrained unmanned aerial vehicles with  
597 recharging on an unmanned ground vehicle. In: *2021 International Conference on Un-*  
598 *manned Aircraft Systems (ICUAS)*, pp. 155–164 (2021). DOI 10.1109/ICUAS51884.2021.  
599 9476848
- 600 24. Rossi, F., Van Beek, P., Walsh, T.: *Handbook of constraint programming*. Elsevier (2006)
- 601 25. Shaw, P., Furnon, V., De Backer, B.: A constraint programming toolkit for local search.  
602 In: *Optimization software class libraries*, pp. 219–261. Springer (2003)
- 603 26. Song, B.D., Kim, J., Morrison, J.R.: Rolling horizon path planning of an autonomous  
604 system of uavs for persistent cooperative service: Milp formulation and efficient heuristics.  
605 *Journal of Intelligent & Robotic Systems* **84**(1-4), 241–258 (2016)
- 606 27. Sundar, K., Venkatachalam, S., Rathinam, S.: Formulations and algorithms for the multi-  
607 ple depot, fuel-constrained, multiple vehicle routing problem. In: *2016 American Control*  
608 *Conference (ACC)*, pp. 6489–6494. IEEE (2016)

- 
- 609 28. Tatsch, C.A.A.: Route Planning for Long-Term Robotics Missions. West Virginia Univer-  
610 sity (2020)
- 611 29. Theile, M., Bayerlein, H., Nai, R., Gesbert, D., Caccamo, M.: UAV coverage path plan-  
612 ning under varying power constraints using deep reinforcement learning. arXiv preprint  
613 arXiv:2003.02609 (2020)
- 614 30. Voudouris, C., Tsang, E.P.: Guided local search. In: Handbook of metaheuristics, pp.  
615 185–218. Springer (2003)
- 616 31. Voudouris, C., Tsang, E.P., Alsheddy, A.: Guided local search. In: Handbook of meta-  
617 heuristics, pp. 321–361. Springer (2010)
- 618 32. Wilkin, G.A., Huang, X.: K-means clustering algorithms: implementation and comparison.  
619 In: Second International Multi-Symposiums on Computer and Computational Sciences  
620 (IMSCCS 2007), pp. 133–136. IEEE (2007)
- 621 33. Younghoon, C., Youngjun, C., Briceno, S., Mavris, D.N.: Energy-constrained multi-uav  
622 coverage path planning for an aerial imagery mission using column generation. Journal of  
623 Intelligent & Robotic Systems **97**(1), 125–139 (2020)